Journal of
Materials Chemistry B

PAPER

View Article Online
View Journal | View Issue

Cite this: J. Mater. Chem. B, 2016, 4, 442

Photo-induced chemistry for the design of oligonucleotide conjugates and surfaces†

Antonina Vigovskaya,[ab] Doris Abt,[bc] Ishtiaq Ahmed,[b] Christof M. Niemeyer,[b] Christopher Barner-Kowollik*[bc] and Ljiljana Fruk*[ad]

Received 22nd October 2015,
Accepted 1st December 2015

DOI: 10.1039/c5tb02207j

www.rsc.org/MaterialsB

A photocaged diene is introduced at the 5′-end of oligonucleotides using the H-phosphonate approach. The photoenol-functionalized DNA is subsequently employed for the conjugation to a protein and the spatially controlled immobilization onto surfaces using a light-induced Diels–Alder cycloaddition. Fully functional protein–DNA conjugates and patterned DNA surfaces are obtained under mild irradiation conditions.

Introduction

Nucleic acids are genetic information carriers, yet due to their structural properties have also found applications as structural elements for the design of nanotechnological constructs,[1–3] used both in the new generation of functional materials[4] or biosensing platforms.[5–7] The range of the possible nucleic acid applications can be extended by introducing various chemical modifications to their structural elements either to prepare different conjugates[8] or to immobilize DNA onto various surfaces.[9–11] To date, a range of strategies has been employed to achieve these aims, including various procedures based on covalent binding[12,13] as well as more specific methods such as cofactor reconstitution.[14] In general, to achieve subsequent conjugation or immobilization, DNA needs to be first modified with the appropriate functional group and the most commonly employed strategy involves addition of such groups to the 5′- and 3′-termini of oligonucleotides as these have no affect on the Watson–Crick base pairing and the stability of the formed double helices,[15] although the modified bases can also be employed for internal labelling of oligonucleotides.[16,17] Functional groups are commonly introduced using standard phosphoramidite chemistry developed by Caruthers and co-workers[18] using DNA synthesis on solid supports.[19] A coupling step involving tetrazole induced activation results in exceptionally high yields and fast coupling reactions. However, the high reactivity is also associated with instability. Thus, phosphoramidites need to be handled carefully and exclusively under inert reaction conditions. Moreover, not all functional groups are compatible with phosphoramidite chemistry.[20] To allow for the addition of specific functional groups, post-synthetic modification of DNA containing thiol or amine moieties is often employed such as the covalent attachment of different species *via* amide coupling or click chemistry procedures.[21,22]

Recently, we have been particularly interested in exploring new photo-induced chemical strategies such as light triggered Diels–Alder cycloadditions[23–26] to design nanoparticle bioconjugates[27] or control the immobilization of various species onto different surfaces such as gold or glass.[28,29] As such types of chemical reaction avoid the use of harsh conditions and as they are controlled by light, they are particularly interesting for surface modification and biointerface design, which can, in turn, be employed for the synthesis of bioinspired materials.[30] Herein, we present the preparation of oligonucleotides modified with hydroxyl-*o*-quinodimethanes (photoenol, PE) and their use for both the preparation of DNA–protein conjugates and surface patterning (Scheme 1). To achieve that, a light triggered Diels–Alder conjugation, based on the [4+2] cycloaddition of a PE generated by the photoisomerisation of *o*-methylphenyl ketones or aldehydes, was applied to a range of different dienophiles such as maleimides.[31–33] The photoenol mediated conjugation strategy requires no catalyst and takes place at ambient temperature. Moreover, it offers temporal and spatial control over the cycloaddition reaction as already shown in the case of biomolecule and polymer immobilization onto variable surfaces[34] as well as the functionalization of nanoparticles[29] and proteins.[35]

[a] DFG-Centre for Functional Nanostructures, Karlsruhe Institute of Technology (KIT), Wolfgang-Gaede-Str. 1a, 76131 Karlsruhe, Germany
[b] Institut für Biologische Grenzflächen, Karlsruhe Institute of Technology (KIT), Hermann-von-Helmholtz-Platz 1, 76344 Eggenstein-Leopoldshafen, Germany
[c] Preparative Macromolecular Chemistry, Institut für Technische Chemie und Polymerchemie, Karlsruhe Institute of Technology (KIT), Engesserstr. 18, 76128 Karlsruhe, Germany. E-mail: christopher.barner-kowollik@kit.edu
[d] Department of Chemical Engineering and Biotechnology, University of Cambridge, New Museums Site, Pembroke Street, Cambridge, CB2 3RA, UK. E-mail: lf389@cam.ac.uk

† Electronic supplementary information (ESI) available. See DOI: 10.1039/c5tb02207j

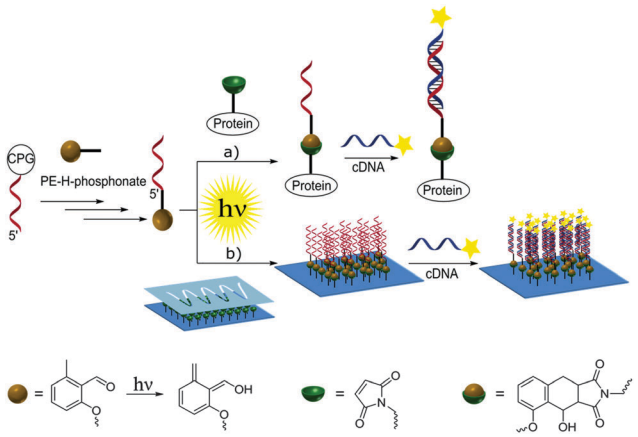

Scheme 1 Introduction of the photoenol moiety into the DNA and subsequent light-induced conjugation to the protein (a) and immobilisation onto the silicon surface as well as hybridisation with the complementary DNA labelled with fluorophore (b).

Experimental

Materials

Triethylene glycol (≥99%, Sigma-Aldrich), anhydrous *N*,*N*-dimethylformamide (DMF, ≥99.8%, Sigma-Aldrich), dichloromethane (DCM, ≥99.8%, VWR), 1-hydroxybenzotriazole hydrate (HOBt, ≥97%, Sigma Aldrich), *N*,*N*-dicyclohexylcarbodiimide (DCC, 99%, Sigma-Aldrich), *N*-hydroxysuccinimide (NHS, 98%, Sigma-Aldrich), methanol (MeOH, 99.8%, VWR), phosphorous acid (H_3PO_3, 99%, Sigma-Aldrich), anhydrous pyridine (99.8%, Sigma-Aldrich), trimethylacetyl chloride (99%, Sigma-Aldrich), acetonitrile (MeCN, 99.9%, VWR), anhydrous acetonitrile (MeCN, 99.8%, Sigma-Aldrich), triethylamine (NEt_3, ≥99%, Sigma-Aldrich), 4-(*N*-maleimidomethyl)cyclohexane-1-carboxylic acid 3-sulfo-*N*-hydroxysuccinimide ester sodium salt (sulfo-SMCC, powder, Sigma-Aldrich), horseradish peroxidase (HRP, type VI-A, Sigma-Aldrich), water (MilliQ (MQ) system, Millipore), oxidizing solution (0.02 M iodine in THF/pyridine/water (7 : 2 : 1), Link Technologies), oligonucleotides **DNA1** and **DNA2** on solid support, **cDNA1**, **6-FAM-cDNA1**, **Cy®3-cDNA1** and **Cy®3-DNA3** (Sigma-Aldrich, for sequences refer to Table S1, ESI†) were used as received. Protein marker, Precision Plus Protein™ Dual Xtra Standards, was purchased from Bio-Rad. DNA marker, O'Range Ruler 10 bp DNA Ladder, was purchased from ThermoFisher Scientific. Triethyl ammonium bicarbonate buffer (TEAB buffer, 2 M, pH 7.5) was prepared by bubbling of gaseous CO_2 into 2 M aqueous solution of triethylamine until the pH of this solution reaches pH 7.5. 4-((2-formyl-3-methyl-phenoxy) methyl) benzoic acid[24] **1**, 2-(2-(2-aminoethoxy)ethoxy)ethan-1-ol[8] **2** and *N*-(2-(2,2-dimethylbenzo[*d*][1,3]dioxol-5-yl)ethyl)-3-(2-(2-(2-(2,5-dioxo-2,5-dihydro-1*H*-pyrrol-1-yl)ethoxy)ethoxy)-ethoxy)-propanamide[36] (**Do-TEG-Mal**) were synthesized according to literature procedures. Gel filtration NAP5 and NAP10 columns and Vivaspin sample concentrators were purchased from GE Healthcare (Germany).

Characterisation

^1H, ^{13}C and ^{31}P NMR spectroscopy was performed using Bruker AM 250, Bruker AM 300 or Bruker AM 400 spectrometer at 250 MHz or 400 MHz respectively. Samples were dissolved in $CDCl_3$ or CD_3CN. The δ-scale is referenced to tetramethylsilane as the internal standard. Fast Atom Bombardment Mass Spectrometry (FAB-MS): the mass spectra were measured using Finnigan MAT90 mass spectrometer. Fast protein liquid chromatography (FPLC) was performed using an Äkta explorer system, which was connected to a MonoQ 5/50 GL anion exchange column (GE Healthcare, Germany). Used purification conditions: buffer A: 20 mM Tris; buffer B: 20 mM Tris, 1 M NaCl; gradient: linear increase of buffer B to 100% in 30 minutes, flowrate: 1 mL min^{-1}, UV/Vis detection at 260 nm and 403 nm. High-performance liquid chromatography (HPLC) was performed using HPLC system 1200 series of Agilent Technologies connected to a Zorbax Eclipse XDB-C18 column (dimensions 4.6 × 150 mm) from Agilent. The following purification conditions were used: (A) 0.1 M NH_4OAc, (B) acetonitrile, gradient 0–100% B over 40 min, flowrate 1 mL min^{-1}, UV/Vis detection at 260 nm and 280 nm. Purification was verified by MS (MALDI-TOF) on a Autoflex III SmartBeam™ (Nd:YAG laser (355 nm) with a repetition rate of 200 Hz) spectrometer from Bruker Daltonics in the linear negative mode; used matrix: a 9 : 1 mixture of saturated 3-hydroxypicolinic acid and 0.44 M diammonium hydrogen citrate. Polyacrylamide gel electrophoresis (PAGE) characterization was performed by using a Mini-Protean® Tetra System, which was connected to a PowerPac™ voltage source (BioRad, Germany). Fourier transform infrared spectra (FTIR) were recorded using Bruker ALPHA and performed in attenuated total reflection (ATR) mode. Time-of-flight secondary ion mass spectrometry (ToF-SIMS) was conducted with a TOF·SIMS[5] instrument (ION-TOF GmbH, Münster, Germany), equipped with a Bi cluster liquid metal primary ion source and a non-linear time-of-flight analyzer. The Bi source was operated in the bunched mode providing 0.7 ns Bi_3^+ ion pulses at 25 keV energy and a lateral resolution of approx. 4 μm. The short pulse length allowed high mass resolution to analyze the complex mass spectra of the immobilized organic layers. Images larger than the maximum deflection range of the primary ion gun of 500 × 500 μm^2 were obtained using the manipulator stage scan mode. Primary ion doses were kept below 10^{11} ions m^{-2} (static SIMS limit). Spectra were calibrated on the CH^-, CH_2^-, CH_3^-, or on the C^+, CH^+, CH_2^+, and CH_3^+ peaks. Fluorescence microscopy was performed using an Axiovert 200 M (Carl Zeiss) inverted microscope with Plan-Neofluar objective (magnification/numeric aperture 5×/0.16).

Synthesis of PE H-phosphonate 4

Synthesis of 3. The synthesis was performed under inert conditions using the literature procedure.[37] The solution of 100 mg (370 μmol, 1.00 eq.) 4-((2-formyl-3-methyl-phenoxy)-methyl)benzoic acid **1** and 51.0 mg (377 μmol, 1.02 eq.) HOBt in 10 mL dry DMF was stirred for 10 minutes at ambient temperature. 78.0 mg (377 μmol, 1.02 eq.) DCC in 5 mL dry

DMF were added and the solution was stirred for another 10 minutes, before 43.0 mg (377 μmol, 1.02 eq.) NHS in 10 mL dry DMF were added dropwise over a period of 30 minutes. The reaction was continued for 2 hours. The resulting NHS ester was added dropwise to a stirred solution of 61.0 mg (407 μmol, 1.10 eq.) 2-(2-(2-aminoethoxy)ethoxy)ethan-1-ol **2** in 10 mL dry DMF over a period of 45 minutes. The reaction mixture was stirred for 48 h at ambient temperature. The urea side product was removed by filtration and the crude product was transferred to chloroform. The organic solution was washed several times with saturated NaCl solution and deionized water. The organic phase was dried over Na_2SO_4 and the solvent was removed *in vacuo*. The crude product was purified by silica gel chromatography, CH/EtOAc (3 : 1, 1 : 1, 1 : 2 (v/v), MeOH), R_f = 0.14 (EtOAc), to give the title compound **3** as yellow solid (yield: 69.8 mg, 47%) (refer to ESI,† for IR, NMR and MS data, Fig. S1 and S2).

Synthesis of 4. 4-((2-Formyl-3-methylphenoxy)methyl)-*N*-(2-(2-(2-hydroxy-ethoxy)ethoxy)-ethyl)benzamide **3** 120 mg (299 μmol, 1.00 eq.) was dissolved in a solution of 1 M phosphorous acid in anhydrous pyridine (9.80 ml, 8.31 mmol of H_3PO_3). Pivaloyl chloride (202 μL, 1.64 mmol, 5.50 eq.) was added dropwise to the reaction mixture. The solution became briefly opaque and was stirred for a further 2 hours. Once complete, the reaction mixture was quenched by addition of TEAB buffer (8.40 mL, 2 M, pH 7.7) and was then extracted twice with DCM. The organic layers were combined and dried over Na_2SO_4. The solvents were removed *in vacuo* to give product **4** as a yellow thick oil, which was used in the next step without further purification. **^{31}P-NMR** (101 MHz, CD_3CN): δ (ppm) = 3.78 (s, 1 P) (Fig. S3, ESI†).

Synthesis of PE-DNA1. The commercial dimethoxytrityl (DMT) protected oligonucleotide (175 nmol) on controlled pore glass (CPG) solid support was deprotected with dichloroacetic acid. The reaction completion was followed by a color change from orange-yellow to colorless. The solid support was washed several times with acetonitrile, dried and transferred to a previously silanized flask. The PE H-phosphonate **4** was dissolved in dry CH_3CN/pyridine (1 : 1, v/v) (33.4 mg, 0.36 M) under argon atmosphere and added to the CPG. Pivaloyl chloride (250 μL, 100 mM in dry CH_3CN/pyridine (1 : 1, v/v)) was added and the reaction mixture was stirred at 39 °C for 16 hours. The reaction solution was removed by centrifugation and the solid support washed with CH_3CN (1 mL × 3). After treatment with standard DNA synthesis oxidizing solution for 3 minutes the CPG was again washed with CH_3CN (1 mL × 3). The PE-modified sequence was deprotected and cleaved from the solid support by incubation with 500 μL 25% ammonia solution at 55 °C for 5 hours. The supernatant was collected and the solvents removed *in vacuo*. Photoenol modified oligonucleotide was dissolved in water and purified by reversed phase HPLC using C18 column (eluent A: 0.100 M ammonium acetate, eluent B: CH_3CN). The main fractions were collected, concentrated *in vacuo* and characterized by MALDI-TOF and PAGE (Fig. S4–S6, ESI†).

General procedure for the photo-induced reactions

The samples to be irradiated were crimped air-tight in headspace vials (20 mm, VWR, Germany) using SBR seals (VWR, Germany) with PTFE inner liner. The photoreactions were performed in a custom-built photoreactor (Fig. S7, ESI†), consisting of a metal disk which revolves at a distance of 40–50 mm around a compact low-pressure fluorescent lamp with λ_{max} = 320 nm ± 30 nm (36 W, Armed B6, Cosmedico GmbH, Germany) (Fig. S8, ESI†). For the spatially controlled surface immobilization of **PE-DNA1**, maleimide functionalized surfaces were mounted into sample holders with a shaddow mask before being immersed with the reaction solution.

Photoreaction between PE-DNA1 and Do-TEG-Mal

The mixture of 2.00 nmol **PE-DNA1** and 2.00 nmol **Do-TEG-Mal** in 1.00 mL H_2O/CH_3CN (1 : 1, v/v) was placed into the headspace vial, which was crimped air-tight as described above, degassed by purging with nitrogen for 15 minutes and subsequently irradiated for 16 hours in the photoreactor at λ_{max} = 320 nm. After the irradiation solvents were removed under reduced pressure, the residue was redissolved in water and purified by reversed phase HPLC using C18 column (eluent A: 0.100 M ammonium acetate, eluent B: CH_3CN). The collected fractions were characterized by MALDI-TOF and native PAGE (Fig. S9 and S10, ESI†).

Photoreaction between PE-DNA1 and HRP-Mal

First **HRP** was functionalized with a maleimide group in the coupling reaction with sulfo-SMCC. Sulfo-SMCC (2.00 mg, 4.58 μmol) was dissolved in 100 μL DMF and added to 200 μL **HRP** solution (166 μM in PBS buffer, pH 6.0) and incubated for 1 hour at ambient temperature. The excess sulfo-SMCC was removed by filtration of the reaction mixture through NAP5 and NAP10 columns. The buffer was exchanged using PBS buffer pH 7.1 as eluent. For the photoreaction 2.00 nmol of **PE-DNA1** and 2.20 nmol of fresh prepared **HRP-Mal** were dissolved in 500 μL of PBS/CH_3CN solution (3 : 2, v/v) and placed into the headspace vial, which was crimped air-tight as described above, degassed by purging with nitrogen for 15 minutes and subsequently irradiated for 16 hours in the photoreactor at λ_{max} = 320 nm. The reaction mixture was filtered through NAP5 and NAP10 columns to exchange the buffer to 20 mM Tris/HCl pH 8.3, concentrated by using 5 kDa Vivaspin and purified by anion exchange chromatography using MonoQ 5/50 GL column (buffer A: 20 mM Tris, buffer B: 20 mM Tris, 1 M NaCl; gradient: linear increase of buffer B to 100% in 30 minutes, flowrate: 1 mL min^{-1}). The concentration and buffer exchange to PBS of the collected fractions were carried out by using 5 kDa Vivaspin, and the characterisation of product fraction was performed by native PAGE.

Spatially controlled surface functionalisation with PE-DNA1 and subsequent hybridization with complementary DNA labelled with Cy®3 dye (Cy®3-cDNA1)

In a headspace vial (Pyrex, diameter 20 mm) 7 nmol **PE-DNA1** were dissolved in 4 mL of PBS/ACN (1 : 1) mixture. Maleimide functionalized silicon surface mounted into the sample holder with mask was placed into the **PE-DNA1** solution. The vial was crimped air-tight using SBR seals with PTFE inner liner.

The solution was deoxygenated by purging with nitrogen for 15 min and subsequently irradiated for 5 h in the photoreactor. After irradiation, the mask was removed. The surface was rinsed with MQ water and sonicated 10 seconds in water to remove any possibly physisorbed material. The surface was subsequently washed with PBS buffer, MQ water, DMF, DMSO, again with MQ water and finally dried under a nitrogen stream. The surface was then analyzed by ToF-SIMS. For the control experiment the same procedure as described above was applied for the non-modified **DNA1**. ToF-SIMS images show no fragments corresponding to **DNA1** (refer to Fig. S16, ESI†). For the hybridization experiments, the surface with immobilized **PE-DNA1** was covered with a 50 μM solution of complementary **DNA** labeled with Cy®3 dye (λ_{Exc} = 550 nm, λ_{Em} = 570 nm) in TETBS buffer (pH = 7.5) and incubated overnight in the dark at ambient temperature. The surface was then washed several times with MQ water, TETBS buffer and again with MQ water, dried under a nitrogen stream and analyzed by fluorescence microscopy. For the control experiment, the surface with immobilized **PE-DNA1** was covered with non-complementary DNA labeled with Cy®3 dye using the same procedure as described above. No fluorescence pattern corresponding to the mask features could be detected (refer to Fig. S17, ESI†).

Results and discussion

Previously, we have used amide coupling of photoenol carboxylic acid to amine modified DNA to prepare photoenol-functional DNA.[35] However, such coupling reactions usually result in minute amounts of functional DNA and involve several steps, which can be circumvented by direct coupling of the PE to the 5′-end of the oligonucleotide during the solid-phase synthesis. To achieve a direct coupling, we decided to employ an H-phosphonate-based strategy instead of commonly used phosphoramidites, as H-phosphonates are easier to handle and more resistant towards oxidation than other P(III) compounds, due to the absence of the lone electron pair located on the phosphorus atom (a consequence of the tetrahedral geometry of H-phosphonates, which contain a phosphoryl group (P═O) and a hydrogen atom bound to the phosphorus centre).[38] First reports on the use of H-phosphonate in nucleotide chemistry originated in the 1950s,[39] yet their use in solid phase synthesis was only demonstrated three decades later by Garegg *et al.*[40] as well as Froehler and Matteucci.[41]

The PE functional H-phosphonate **4** is prepared as shown in Fig. 1. In the first step, an OH group containing precursor is required to enable the subsequent reaction with P(III) compounds (*e.g.*, H_3PO_4 or PCl_3) in order to afford an H-phosphonate derivative. Therefore, we have first prepared PE **3** containing a PE function and a three membered glycol unit to allow for more steric freedom for the following ligation. Subsequently, the PE H-phosphonate **4** was directly obtained from PE **3** using the modified procedure described by Dougan and co-workers.[20] The PE modified oligonucleotide sequences **DNA1** and **DNA2** were obtained by direct coupling to commercially available

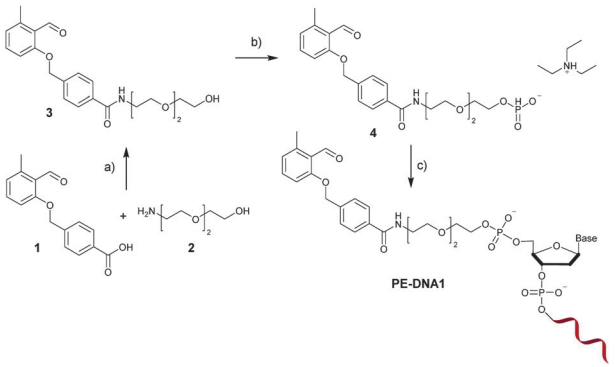

Fig. 1 Synthesis of the photoenol containing oligonucleotide **PE-DNA1**: (a) HOBt, DCC, NHS, DMF, r.t., 48 h, 47%; (b) H_3PO_3, pivaloyl chloride, pyridine, r.t., 2 h, TEAB buffer; (c) solid phase synthesis.

CPG-bound oligonucleotides using the PE-H-phosphonate **4** and pivaloyl chloride as activator. The products, **PE-DNA1** and **PE-DNA2**, were purified using reversed phase HPLC and identified by MALDI-TOF mass spectrometry (Fig. S4 and S5, ESI†). Gel electrophoresis was additionally used for the characterisation of both **PE-DNAs** (Fig. S6, ESI†).

To allow for the light-induced cycloaddition, irradiation of PE oligonucleotides with a UVA lamp (λ_{max} = 320 nm) in the presence of maleimide containing molecules of interest is needed. Previous reports have shown that the UV irradiation with the same wavelength of non-modified DNA in PBS/CH_3CN (1 : 1) had no destructive effect on the functionality of the oligonucleotide.[35] In order to investigate the influence of the irradiation on the PE modified oligonucleotide, a proof of concept reaction was initially performed by irradiating **PE-DNA1** in the presence of the maleimide containing molecule **Do-TEG-Mal** (Fig. 2). The HPLC purification and subsequent analysis by gel electrophoresis and MALDI-TOF showed that the reaction was successful and the desired product was obtained (Fig. S9, ESI†). In addition, PE-DNA2 with a different sequence was used for the reaction, indicating that the light induced photoenol reaction is not sequence specific (Fig. S10, ESI†).

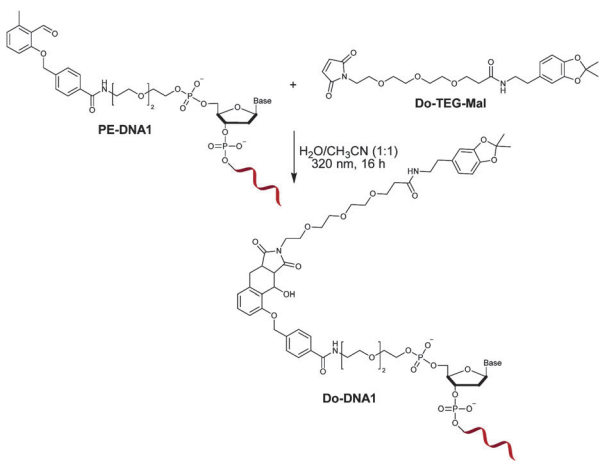

Fig. 2 Light-induced conjugation of **PE-DNA1** and **Do-TEG-Mal**.

When the reaction is performed using non-modified DNA, no product was obtained (Fig. S11, ESI†).

Furthermore, a control reaction was carried out by irradiating **PE-DNA1** alone. Here, some signals with shorter retention time and lower absorption intensity were detected during HPLC (refer to Fig. S12, ESI†), indicating that there are possible side reactions of the photoenol moiety and the nucleobases upon UV irradiation, most probably with available amine groups. However, photoreactions in the presence of the dienophile **Do-TEG-Mal** revealed the desired **Do-DNA1** cycloadduct as the main product (refer to Fig. S12, ESI†) evidenced by HPLC analysis as well as by MALDI-TOF (refer to Fig. S9, ESI†). Furthermore, an additional control experiment was carried out in which **PE-DNA1** and **Do-TEG-Mal** were incubated overnight in the absence of light, showing that there is no significant amount of product or side products formed (refer to Fig. S12, ESI†).

It should be noted that overnight irradiation was performed to ensure the maximum conversion of the starting material to the cycloadduct in aqueous solution, as protic solvents favor the reconversion of dienol species to ketone/aldehyde tautomers.[24,42] As reported by Tchir and Porter, five transients have been observed *via* laser flash photolysis of 2,4-dimethylbenzophenone in cyclohexane or ethanol.[43] The dienol intermediate exists as a mixture of two isomers (*E*- and *Z*-isomer). The *Z* isomer decays much faster than the *E* isomer. Measured lifetimes of the dienols in cyclohexane were 4 s for the *Z*- and 250 s for the *E*-dienol. Arnold *et al.* described a similar photochemical process for 2-methylbenzaldehyde, where the *E*- and *Z*-dienols are the expected initial products.[44] The lifetimes of these dienols are not reported, yet the authors claim that the cycloaddition reaction with a dienophile is efficient and depends on the rate of dienol formation.

To demonstrate that the photo-induced cycloaddition of PE modified oligonucleotide can further be employed in more complex applications, protein–DNA conjugates using maleimide containing horseradish peroxidase (**HRP-Mal**) were prepared. **HRP** is a biotechnologically very important protein and one of the most potent peroxidases.[45] As proteins are, in general, sensitive to UV light, the effect of prolonged irradiation was first assessed by irradiating native **HRP** with λ_{max} = 320 nm light overnight. SDS-PAGE analysis showed neither a difference in electrophoretic mobility between irradiated and non-irradiated **HRP** nor additional fragments for irradiated samples (Fig. S15, ESI†), indicating that there is no significant structural damage of the protein under the employed irradiation conditions. For the preparation of protein–DNA conjugates, the mixture of **HRP-Mal** and **PE-DNA1** was irradiated in PBS/CH_3CN (3 : 2) overnight (Fig. 3a), purified by fast protein liquid chromatography (Fig. 3b) and analyzed by gel electrophoresis (Fig. 3c). The gel characterization showed that the peak F1 represents the non-modified **HRP-Mal**. The peak F2 was assigned to the **HRP–DNA1** photoconjugate, as it shows the higher electrophoretic mobility in comparison to **HRP** and **HRP-Mal** due to the increased negative charge after the coupling to **PE-DNA1**. In addition, the presence of the oligonucleotide in the **HRP–DNA1**

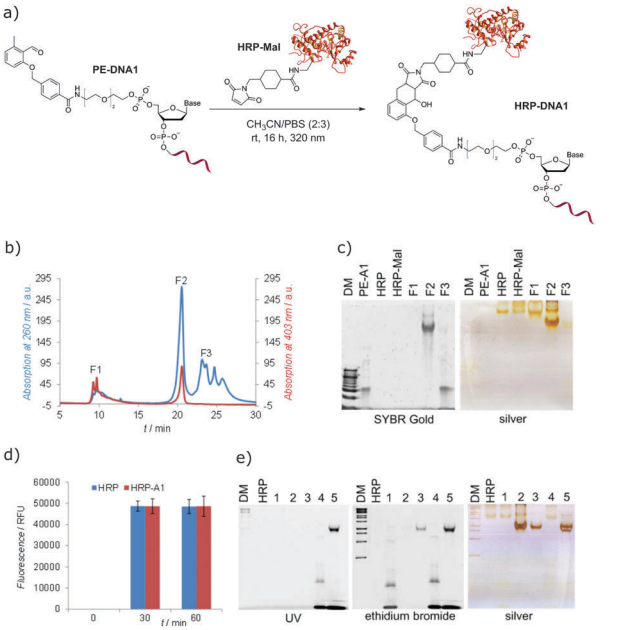

Fig. 3 (a) Photo-triggered conjugation of **PE-DNA1** and maleimide functionalized HRP (**HRP-Mal**); (b) FPLC chromatogram of the **HRP–DNA1** purification; (c) native PAGE characterization of the FPLC fractions F1, F2 and F3; oligonucleotide/protein visualization by SYBR Gold/silver staining; DM: 10 bp DNA-marker; (d) fluorescence **HRP** activity assay; (e) native PAGE analysis of hybridization of **HRP–DNA1** with complementary strands **cDNA1** and **6-FAM-cDNA1**, DM: 1 kb DNA-marker, HRP: native **HRP**; (1) negative control (**HRP** + **DNA1** + **cDNA1** or (4) **HRP** + **DNA1** + **6-FAM-cDNA1**), (2) **HRP–DNA1** conjugate, (3) **HRP–DNA1** + **cDNA1**, (5) **HRP–DNA1** + **6-FAM-cDNA1**; visualization: UV irradiation, ethidium bromide and silver staining.

fraction was evidenced by SYBR Gold staining. Fraction F3 represents the non-reacted **PE-DNA1**. In order to explore if any non-specific side reactions take place between modified and unmodified **HRP** and **DNA1**, a set of control reactions was performed (Fig. S13, ESI†). In case of the reaction between native **HRP** and **PE-DNA1** under irradiation, a small amount of conjugate could be detected in the FPLC chromatogram, indicating the occurrence of a reaction of the photoenol moiety with the protein – possibly with free lysine groups. However, the significant amount of the conjugate obtained in the photoreaction of **HRP-Mal** and **PE-DNA1** shows that the photoenol-mediated cycloaddition is preferred (Fig. S14, ESI†). The selectivity of the photoreaction was additionally confirmed by the absence of conjugate after the incubation of **HRP-Mal** and **PE-DNA1** in the dark as well as in case of irradiation of **PE-DNA1** with **HRP** or with **HRP-Mal** (Fig. S13, ESI†).

In order to investigate if the inherent functions of **HRP** and DNA are preserved in the **HRP–DNA1** conjugate, the peroxidase activity of **HRP** and the hybridization ability of DNA were tested. The Amplex®Red assay was used to assess the peroxidase activity of the **HRP–DNA1** conjugate, employing the conversion of non-fluorescent substrate Amplex Red into fluorescent resorufin in the presence of peroxidase enzymes and H_2O_2 (Scheme S2, ESI†). Fluorescence measurements (Fig. 3d) showed similar results for native **HRP** and **HRP–DNA1** conjugate

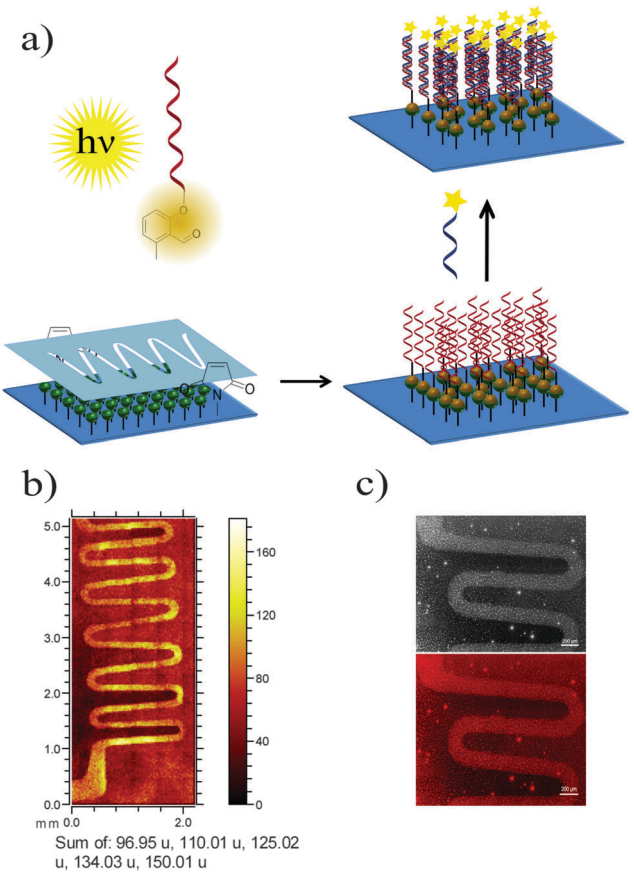

Fig. 4 (a) Light-induced DNA immobilization with spatial resolution; (b) ToF-SIMS imaging of photo-patterned **PE-DNA1** derived from the sum of the signals detected at 96.95 ($H_2PO_4^-$), 150.01 (G^-), 125.02 (T^-), 134.03 (A^-) and 110.01 (C^-) assigned to fragments of the corresponding oligonucleotides; (c) fluorescence microscopy of hybridized **cDNA1-Cy®3** on the surface patterned with **PE-DNA1** (top: grey scale image, bottom: Cy®3 fluorescence image).

indicating the high peroxidase activity of the conjugate. For the hybridization ability test, the **HRP–DNA1** conjugate was incubated with a 10-fold excess of **cDNA1** and 6-FAM dye labelled **cDNA1**. As shown in Fig. 3e, hybridization success was confirmed by detection of 6-FAM fluorescence after UV irradiation, ethidium bromide and silver staining. Further, as negative controls, native **HRP** was incubated with **DNA1**, **cDNA1** and with **6-FAM-cDNA1** and no **HRP** mobility shifts or fluorescence bands indicating the hybridization were observed after the ethidium bromide staining and UV irradiation.

The ability of 5′-photoenol-modified oligonucleotides to undergo a light-induced cycloaddition reaction with maleimide functionalized molecules in solution prompted us to employ it for the temporally and spatially controlled patterning of oligonucleotides and the design of functional material-biomolecule interfaces. Thus, we initially functionalized a silicon surface with maleimide groups using a previously reported procedure.[46] The spatial control was achieved by utilizing a shadow mask with wave patterns (Fig. 4a).[47] The maleimide functionalized silicon wafer, covered with a shadow mask, was irradiated in a solution of **PE-DNA1** in PBS/CH_3CN (1 : 1) for 5 hours. The control experiment was performed *via* the irradiation of non-modified **DNA1** under the same reaction conditions. One issue that may arise upon surface modification is the formation of a potential self-adduct between two identical enol species, decreasing the efficiency of the DNA immobilisation. However, as reported by Arnold *et al.*, the dimer formation between two 2-methylbenzaldehyde molecules could be detected at relatively high concentration (*ca.* 0.1 M) conditions.[44] The dimerisation reaction in more diluted solutions (0.003 M) was found to be, however, disfavored. In our current study, solutions with less than 4 μM concentrations of enol species were employed, therefore the dimerisation reaction is not expected. In any case, even if dimerization has occurred, the dimers will not be attached to the surface and are washed off.

The surfaces patterned with oligonucleotides were analyzed by time-of-flight secondary ion mass spectrometry (ToF-SIMS). Fig. 4b depicts the ToF-SIMS image resulting from the sum of characteristic species assigned to nucleic acids of DNA (m/z = 96.95 ($H_2PO_4^-$), 150.01 (G^-, guanine), 125.02 (T^-, thymine), 134.03 (A^-, adenine) and m/z = 110.01 (C^-, cytosine))[48] immobilized in a patterned fashion following the mask's features.

Once it had been shown that **PE-DNA1** was successfully immobilized, we assessed if the surface bound **DNA1** remained functional after irradiation. Thus, surfaces patterned with DNA were incubated with complementary oligonucleotide **cDNA1** labelled with a commercially available fluorophore Cy®3 (λ_{Exc} = 550 nm, λ_{Em} = 570 nm). The fluorescence detection of hybridized oligonucleotides was performed by fluorescence microscopy and shows a clear fluorescent pattern in the areas with immobilized **DNA1** (Fig. 4c). The overnight hybridization leads to some limited aggregation of the cDNA1-Cy®3 and a subsequent adsorption of the aggregates onto the surfaces. The aggregates are visible as very small circular deposits in the non-irradiated areas of the array. Further optimization of the hybridization patterns is required. However, a clear fluorescent pattern was visible indicating successful DNA immobilization and subsequent hybridization, therefore allowing for future immobilisation of various species through DNA directed immobilization.

Conclusions

We have introduced a facile route to prepare 5′-photoenol-modified oligonucleotides *via* an H-phosphonate solid phase coupling method. The approach has proven to be a useful tool for oligonucleotide modification with a photocaged diene species which can further react with dienophiles such as functional maleimide using a light-induced [4+2] cycloaddition reaction. Employing photo-triggered reactions both protein–DNA (HRP–DNA) conjugates and patterned DNA surfaces were prepared. We believe that the introduced methodology can be readily expanded further for the controlled assembly of oligonucleotides onto structured surfaces to create, *e.g.*, catalytic centres within artificial enzymes. Our further efforts

are focused on designing a library of different photoenol species, which in the future will enable photoorthogonal DNA assembly.

Acknowledgements

The current study was supported by DFG-CFN grant A 5.7. C. B.-K. and C. M. N. acknowledge continued support from the Karlsruhe Institute of Technology (KIT) in the context of the Helmholtz programme BioInterfaces in Technology and Medicine (BIFTM). A. V. thanks Annette Hochgesand (KIT) for the MALDI-TOF measurements.

References

1 Y. C. Hung, D. M. Bauer, I. Ahmed and L. Fruk, *Methods*, 2014, **67**, 105–115.
2 O. I. Wilner and I. Willner, *Chem. Rev.*, 2012, **112**, 2528–2556.
3 C. Geary, P. W. Rothemund and E. S. Andersen, *Science*, 2014, **345**, 799–804.
4 A. Kuzuya and M. Komiyama, *Nanoscale*, 2010, **2**, 310–322.
5 B. Hotzer, I. L. Medintz and N. Hildebrandt, *Small*, 2012, **8**, 2297–2326.
6 D. G. Thompson, A. Enright, K. Faulds, W. E. Smith and D. Graham, *Anal. Chem.*, 2008, **80**, 2805–2810.
7 C. S. Thaxton, R. Elghanian, A. D. Thomas, S. I. Stoeva, J. S. Lee, N. D. Smith, A. J. Schaeffer, H. Klocker, W. Horninger, G. Bartsch and C. A. Mirkin, *Proc. Natl. Acad. Sci. U. S. A.*, 2009, **106**, 18437–18442.
8 D. M. Bauer, I. Ahmed, A. Vigovskaya and L. Fruk, *Bioconjugate Chem.*, 2013, **24**, 1094–1101.
9 G. Shtenberg, N. Massad-Ivanir, O. Moscovitz, S. Engin, M. Sharon, L. Fruk and E. Segal, *Anal. Chem.*, 2013, **85**, 1951–1956.
10 G. Shtenberg, N. Massad-Ivanir, S. Engin, M. Sharon, L. Fruk and E. Segal, *Nanoscale Res. Lett.*, 2012, **7**, 443.
11 H. Schroeder, M. Adler, K. Gerigk, B. Muller-Chorus, F. Gotz and C. M. Niemeyer, *Anal. Chem.*, 2009, **81**, 1275–1279.
12 L. Fruk, J. Muller, G. Weber, A. Narvaez, E. Dominguez and C. M. Niemeyer, *Chem. – Eur. J.*, 2007, **13**, 5223–5231.
13 C. M. Niemeyer, *Angew. Chem., Int. Ed.*, 2010, **49**, 1200–1216.
14 L. Fruk and C. M. Niemeyer, *Angew. Chem., Int. Ed.*, 2005, **44**, 2603–2606.
15 G. N. Grimm, A. S. Boutorine and C. Helene, *Nucleosides, Nucleotides Nucleic Acids*, 2000, **19**, 1943–1965.
16 L. Fruk, A. Grondin, W. E. Smith and D. Graham, *Chem. Commun.*, 2002, 2100–2101.
17 I. K. Astakhova and J. Wengel, *Chem. – Eur. J.*, 2013, **19**, 1112–1122.
18 S. L. Beaucage and M. H. Caruthers, *Tetrahedron Lett.*, 1981, **22**, 1859–1862.
19 S. Roy and M. Caruthers, *Molecules*, 2013, **18**, 14268–14284.
20 J. A. Dougan, A. K. Reid and D. Graham, *Tetrahedron Lett.*, 2010, **51**, 5787–5790.
21 P. M. Gramlich, S. Warncke, J. Gierlich and T. Carell, *Angew. Chem., Int. Ed.*, 2008, **47**, 3442–3444.
22 M. Shelbourne, T. Brown, Jr., A. H. El-Sagheer and T. Brown, *Chem. Commun.*, 2012, **48**, 11184–11186.
23 K. K. Oehlenschlaeger, J. O. Mueller, N. B. Heine, M. Glassner, N. K. Guimard, G. Delaittre, F. G. Schmidt and C. Barner-Kowollik, *Angew. Chem., Int. Ed.*, 2013, **52**, 762–766.
24 T. Pauloehrl, G. Delaittre, V. Winkler, A. Welle, M. Bruns, H. G. Borner, A. M. Greiner, M. Bastmeyer and C. Barner-Kowollik, *Angew. Chem., Int. Ed.*, 2012, **51**, 1071–1074.
25 A. S. Quick, H. Rothfuss, A. Welle, B. Richter, J. Fischer, M. Wegener and C. Barner-Kowollik, *Adv. Funct. Mater.*, 2014, **24**, 3571–3580.
26 K. Hiltebrandt, T. Pauloehrl, J. P. Blinco, K. Linkert, H. G. Borner and C. Barner-Kowollik, *Angew. Chem., Int. Ed.*, 2015, **54**, 2838–2843.
27 L. Stolzer, A. Vigovskaya, C. Barner-Kowollik and L. Fruk, *Chem. – Eur. J.*, 2015, **21**, 14309–14313.
28 L. Stolzer, A. S. Quick, D. Abt, A. Welle, D. Naumenko, M. Lazzarino, M. Wegener, C. Barner-Kowollik and L. Fruk, *Chem. Commun.*, 2015, **51**, 3363–3366.
29 L. Stolzer, I. Ahmed, C. Rodriguez-Emmenegger, V. Trouillet, P. Bockstaller, C. Barner-Kowollik and L. Fruk, *Chem. Commun.*, 2014, **50**, 4430–4433.
30 C. M. Preuss, T. Tischer, C. Rodriguez-Emmenegger, M. M. Zieger, M. Bruns, A. S. Goldmann and C. Barner-Kowollik, *J. Mater. Chem. B*, 2014, **2**, 36–40.
31 J. L. Charlton and M. M. Alauddin, *Tetrahedron*, 1987, **43**, 2873–2889.
32 S. M. Mellows and P. G. Sammes, *J. Chem. Soc. D*, 1971, 21–22.
33 T. Gruendling, K. K. Oehlenschlaeger, E. Frick, M. Glassner, C. Schmid and C. Barner-Kowollik, *Macromol. Rapid Commun.*, 2011, **32**, 807–812.
34 G. Delaittre, A. S. Goldmann, J. O. Mueller and C. Barner-Kowollik, *Angew. Chem., Int. Ed.*, 2015, **54**, 11388–11403.
35 D. M. Bauer, A. Rogge, L. Stolzer, C. Barner-Kowollik and L. Fruk, *Chem. Commun.*, 2013, **49**, 8626–8628.
36 C. Chen, I. Ahmed and L. Fruk, *Nanoscale*, 2013, **5**, 11610–11614.
37 T. D. Schladt, K. Schneider, M. I. Shukoor, F. Natalio, H. Bauer, M. N. Tahir, S. Weber, L. M. Schreiber, H. C. Schroder, W. E. G. Muller and W. Tremel, *J. Mater. Chem.*, 2010, **20**, 8297–8304.
38 A. Kraszewski and J. Stawinski, *Pure Appl. Chem.*, 2007, **79**, 2217–2227.
39 N. S. Corby, G. W. Kenner and A. R. Todd, *J. Chem. Soc.*, 1952, 3669–3675.
40 P. J. Garegg, I. Lindh, T. Regberg, J. Stawinski, R. Stromberg and C. Henrichson, *Tetrahedron Lett.*, 1986, **27**, 4051–4054.
41 B. C. Froehler and M. D. Matteucci, *Tetrahedron Lett.*, 1986, **27**, 469–472.
42 P. G. Sammes, *Tetrahedron*, 1976, **32**, 405–422.
43 G. Porter and M. F. Tchir, *J. Chem. Soc. D*, 1970, 1372–1373.
44 B. J. Arnold, S. M. Mellows, P. G. Sammes and T. W. Wallace, *J. Chem. Soc., Perkin Trans. 1*, 1974, 401–409.

45 F. W. Krainer and A. Glieder, *Appl. Microbiol. Biotechnol.*, 2015, **99**, 1611–1625.
46 B. Yameen, C. Rodriguez-Emmenegger, C. M. Preuss, O. Pop-Georgievski, E. Verveniotis, V. Trouillet, B. Rezek and C. Barner-Kowollik, *Chem. Commun.*, 2013, **49**, 8623–8625.
47 T. Tischer, T. K. Claus, M. Bruns, V. Trouillet, K. Linkert, C. Rodriguez-Emmenegger, A. S. Goldmann, S. Perrier, H. G. Borner and C. Barner-Kowollik, *Biomacromolecules*, 2013, **14**, 4340–4350.
48 L. E. Cheran, D. Vukovich and M. Thompson, *Analyst*, 2003, **128**, 126–129.